1986

Methyl and Tert-Butyl Reorientation and Distributions of Activation Energies in Molecular Solids: A Nuclear Spin-Relaxation Study in 2,4- and 2,5-Di-Tert-Butylhydroxybenzene

Peter A. Beckmann
Bryn Mawr College, pbeckman@brynmawr.edu

A. M. Cheung

E. E. Fisch

F. A. Fusco

R. E. Herzog

See next page for additional authors

Authors

Peter A. Beckmann, A. M. Cheung, E. E. Fisch, F. A. Fusco, R. E. Herzog, and M. Narisimhan

Methyl and *tert*-butyl reorientation and distributions of activation energies in molecular solids. A nuclear spin-relaxation study in 2,4- and 2,5-di-*tert*-butylhydroxybenzene

P. A. Beckmann, A. M. Cheung,[a] E. E. Fisch,[b] F. A. Fusco,[c] R. E. Herzog,[d] and
M. Narasimhan[e]

Department of Physics, Bryn Mawr College, Bryn Mawr, Pennsylvania 19010

We have measured proton Zeeman relaxation rates R in the 2,4- and 2,5-isomers of di-*tert*-butylhydroxybenzene (DTHB) in the solid state. R was measured as a function of temperature T at proton Larmor frequencies of $\omega/2\pi = 8.50$, 22.5, and 53.0 MHz. The T ranges were from 78 K to just below the melting points of 2,4- and 2,5-DTHB, 385 and 323 K, respectively. The 2,5-DTHB R vs T and ω can be interpreted qualitatively in terms of three Bloembergen–Purcell–Pound (BPP) spectral densities, one for each of the three types of rotors in the molecule. The quantitative agreement is poor but a good fit is obtained using either a Davidson–Cole (DC) or Frölich spectral density, still preserving the three rotor types. The implications of this are discussed. The BPP and DC spectral densities fail completely in interpreting R vs T and ω for 2,4-DTHB whereas good quantitative fits are obtained using a Frölich spectral density. The distributions of activation energies characterizing the three rotor types are so wide for the Frölich spectral density fit of the 2,4-DTHB data that the individual rotor types lose their identity.

INTRODUCTION

Nuclear spin relaxation[1] is a useful technique to study the reorientational dynamics of intramolecular groups in molecular solids. In this paper we report the temperature and Larmor frequency dependence of the proton Zeeman relaxation rate R in the 2,4- and 2,5-isomers of di-*tert*-butyl-hydroxybenzene (DTHB). The relaxation is dominated by the modulation of the proton dipole–dipole interactions by the reorientations of the *tert*-butyl $[C(CH_3)_3]$ groups and their constituent methyl (CH_3) groups. The molecules, shown schematically in Fig. 1, are similar yet the relaxation rate data in Fig. 2 (2,5-DTHB) and Fig. 3 (2,4-DTHB) are very different. The presence of three relaxation peaks in 2,5-DTHB, along with considerable other supporting evidence, makes the interpretation of which rotors are contributing to the relaxation in the various temperature regions unique.[2] However, quantitative analysis of the 2,5-DTHB data suggests that the correlation functions for intramolecular reor-

ientation are nonexponential either because they are inherently so or because there exists a distribution of electrostatic potentials which manifests itself in a distribution of observed activation energies and correlation times for intramolecular reorientation. The 2,4-DTHB data, although apparently very different from that for 2,5-DTHB, can be interpreted on the basis of the same motions present in 2,5-DTHB. Also, a spectral density of the same form can be used for both isomers though a much broader distribution of correlation times is required for the 2,4-isomer. We discuss these matters following a more detailed presentation of the fundamental theory and the experimental results.

THE EXPERIMENTS

Proton Zeeman relaxation rates R in the 2,5- and 2,4-isomers of di-*tert*-butylhydroxybenzene (DTHB) were measured using standard pulsed NMR techniques. The apparatus and the procedures are discussed elsewhere.[3] Both 2,4-DTHB and 2,5-DTHB were purchased from the Aldrich Chemical Company and were recrystallized three times

---

[a] Part of this work forms part of the requirements for the A.B. degree with Honors (Bryn Mawr College, 1984). Present address: School of Medicine, Johns Hopkins University, 720 Rutland Avenue, Baltimore, MD 21205.

[b] Part of this work forms part of the requirements for the A.B. degree with Honors (Bryn Mawr College, 1985). Present address: Department of Applied Physics, Yale University, New Haven, CT 06520.

[c] Part of this work forms part of the requirements for the A.B. degree with Honors (Bryn Mawr College, 1983). Present address: Department of Materials Science and Engineering, Massachusetts Institute of Technology, Cambridge, Massachusetts 02139.

[d] Part of this work forms part of the requirements for an Undergraduate Unit of Research (Bryn Mawr College, 1984). Present address: Department of Chemical Engineering, Johns Hopkins University, Baltimore, MD 21218.

[e] Part of this work forms part of the requirements for an Undergraduate Unit of Research (Bryn Mawr College, 1985). Present address: School of Medicine, University of Geneva, Geneva, Switzerland.
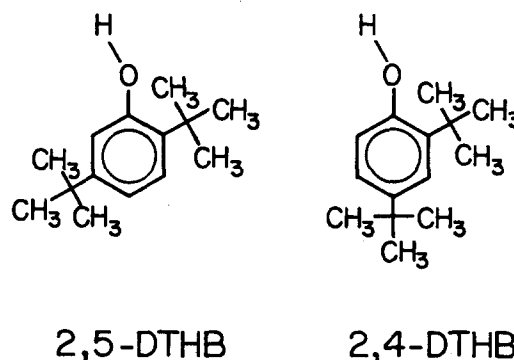
FIG. 1. Schematic structure of the 2,5- and 2,4-isomers of di-*tert*-butylhydroxybenzene abbreviated 2,5-DTHB and 2,4-DTHB, respectively.
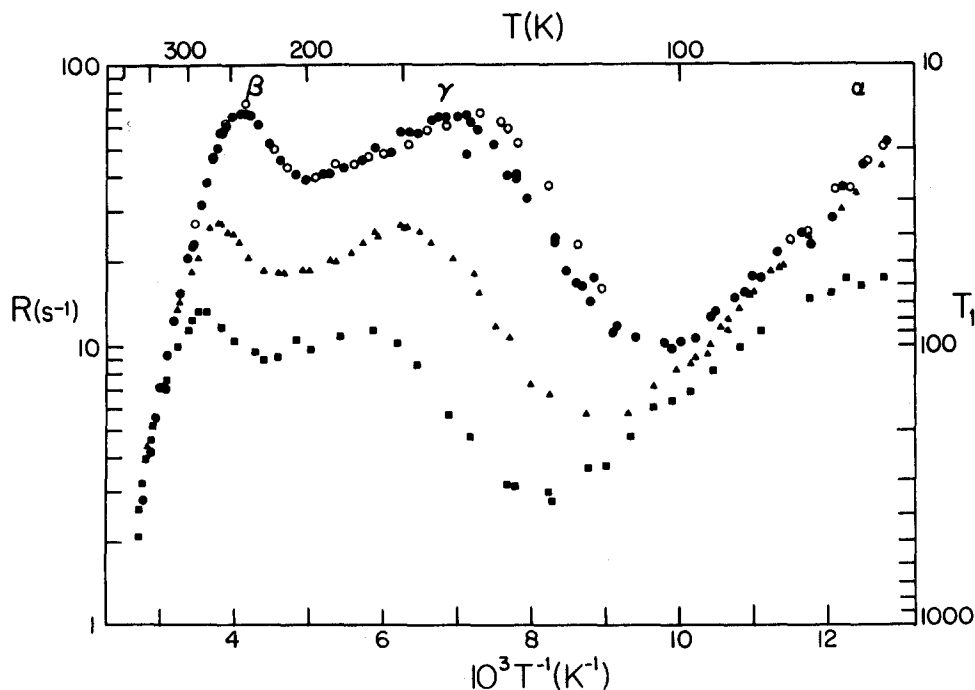
FIG. 2. Measured R vs T in 2,5-DTHB-OD at $\omega/2\pi = 8.50$ (full circles), 22.5 (full triangles), and 53.0 MHz (full squares), and 2,5-DTHB-OH at 8.50 MHz (open circles). The high temperature region is shown on an expanded scale in Fig. 5. The α, β, and γ peaks are referred to in the text.

from 2-propanol. Samples of both molecules were deuterated in the OH position by exchange with 2-propanol-OD. High resolution NMR showed that the deuteration in both isomers was about 85%. Powder samples of 2,5-DTHB-OD were long lived (years) but powder samples of 2,4-DTHB-OD reverted quickly (days) to the fully protonated form.

The R vs T data are shown in Fig. 2 for 2,5-DTHB and 2,5-DTHB-OD, and in Fig. 3 for 2,4-DTHB and 2,4-DTHB-OD. The high temperature data for the 2,5- and 2,4-isomers are shown on expanded scales in Figs. 5 and 12, respectively.
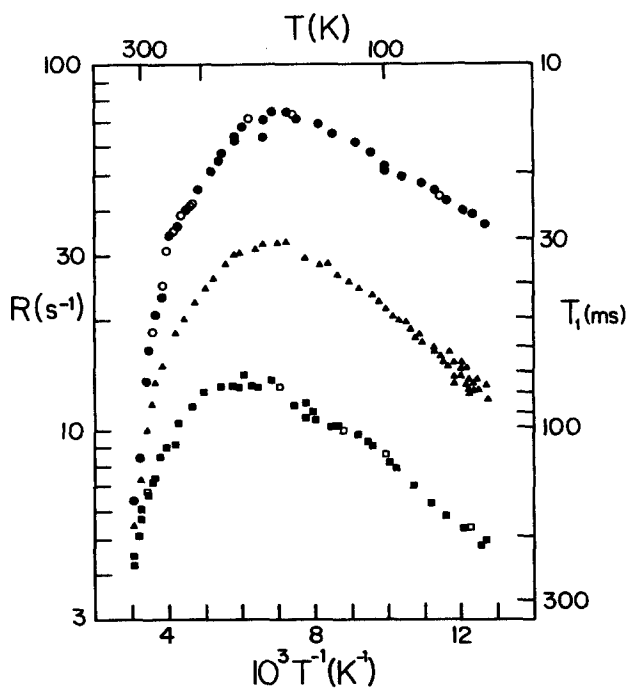

FIG. 3. Measured R vs T in 2,4-DTHB-OD at $\omega/2\pi = 8.50$ (full circles), 22.5 (full triangles), and 53.0 MHz (full squares), and 2,4-DTHB-OH at 8.50 (open circles) and 53.0 MHz (open squares). The high temperature region is shown on an expanded scale in Fig. 12.

Temperature T was varied from liquid nitrogen (77 K) to just below the melting points; 385 K for 2,5-DTHB and 323 K for 2,4-DTHB. R vs T was measured at Larmor frequencies of $\omega/2\pi = 8.50$, 22.5, and 53.0 MHz as indicated in the figures.

A previous introductory study in 2,5-DTHB[4] showed significant thermal history effects. The day to day thermal history was not controlled in this previous study, and a very large scatter in the data resulted. This scatter has been eliminated by recycling the samples between 77 K and room temperature three times before each set of experiments. The same procedure was used with 2,4-DTHB and 2,4-DTHB-OD as well as with 2,5-DTHB and 2,5-DTHB-OD. This resulted in reproducible results over very long periods of time (> one year).

The samples were not sealed but were placed in open sample tubes which were well wrapped with Teflon tape. With this technique, the thermocouple can be inserted inside the sample in a region just outside the coil. It is very important in these studies to have accurate and long term reproducible temperature measurement and that is why this technique was employed. The minimum value of R was $2s^{-1}$, and this is well above the value where paramagnetic impurities such as trapped oxygen are important in solids that have not been liquified following recrystallization. We have discussed the pros and cons of various sample preparation techniques elsewhere.[3,5]

THEORY

We review the derivation of the Zeeman relaxation rate R in systems with *tert*-butyl groups and then specialize this to the case of the present molecules. There are two parts to the problem: the expressions for R in terms of the spectral densities for intramolecular reorientation and the nature of the temperature and Larmor frequency dependence of the spectral densities. The first part requires that the various rotors and their superimposed motions be considered. Al-

though this is tedious, it is straightforward.[2,6,7] The spectral density part involves a detailed knowledge of the dynamical processes and as such is an unsolved problem.

Relaxation in *tert*-butyl systems

The Zeeman relaxation rate in a wide variety of aromatic compounds containing *tert*-butyl groups arises from the modulation of the various dipole–dipole interactions by the intramolecular reorientations.[1] Reorientation of a *tert*-butyl group is characterized by a correlation time τ_2 and the reorientation of a constituent methyl group is characterized by a correlation time τ_3. The intramethyl dipole–dipole interactions are modulated by both these motions and as such the intramethyl relaxation rate contains terms involving τ_2, τ_3, and $\tau_{23} = (\tau_2^{-1} + \tau_3^{-1})^{-1}$. The intramethyl relaxation rate of the jth type of methyl group in the ith type of *tert*-butyl group in a powder sample is given by[2,7]

$$R_{ij}^{\text{intra}} = (3/10) \, C^{\text{intra}} \, [(2/9) \, F(\omega, \tau_3^{ij})$$
$$+ (2/9) \, F(\omega, \tau_2^i) + (19/36) \, F(\omega, \tau_{23}^{ij})] \quad (1)$$

with

$$C^{\text{intra}} = [\mu_0/(4\pi)]^2 \, \gamma^4 \hbar^2/r^6 = 1.69 \times 10^{10} \text{ s}^{-2} \quad (2)$$

and

$$F(\omega, \tau) = j(\omega, \tau) + 4j(2\omega, \tau) . \quad (3)$$

The constants entering C^{intra} are $\mu_0/(4\pi) = 10^{-7}$ m kg s^{-2} A^{-2}, $\hbar = 1.055 \times 10^{-34}$ m^2 kg s^{-1}, the magnetogyric ratio $\gamma = 2.675 \times 10^8$ kg^{-1} s A, and the proton–proton distance in a methyl group, $r = 1.797 \times 10^{-10}$ m. The reduced spectral density $j(\omega, \tau)$ depends on the proton Lamor angular frequency. $\omega = \gamma B$ for an applied magnetic field of magnetic induction B and, at the very least, a correlation time τ which characterizes the motion. In general, additional molecular parameters may be required to characterize $j(\omega, \tau)$.

In addition to intramethyl effects, we include the modulation of dipole–dipole interactions between protons in different methyls within a *tert*-butyl group. Since the distances are time dependent the calculation of this R^{inter} is very difficult[8] but can be approximated by condensing the three protons of a methyl group to the center of their reorientation axis.[9] The system then becomes a fixed triangular group reorienting with a correlation time τ_2. The intermethyl, intra-*tert*-butyl relaxation rate resulting from the modulation of these interactions by the reorientations of the ith type of *tert*-butyl group in a powder sample is[2,7,9]

$$R_i^{\text{inter}} = (3/10) \, C^{\text{inter}} \, [(3/4) \, F(\omega, \tau_2^i)] \quad (4)$$

with

$$C^{\text{inter}} = 3 \, [\mu_0/(4\pi)]^2 \, \gamma^4 \hbar^2/r_*^6 = 1.87 \times 10^9 \text{ s}^{-2} . \quad (5)$$

The distance between methyl groups in this approximation is $r_* = 3.12 \times 10^{-10}$ m and the factor of 3 in C^{inter} accounts for the three spins (a methyl group) at each vertex of the reorienting triangle. The factor 3/4 in Eq. (4) can be compared with the case of $\tau_2 \rightarrow \infty$, $\tau_{23} \rightarrow \tau_3$ in Eq. (1) in which case $F(\omega, \tau_2) \rightarrow 0$, $F(\omega, \tau_{23}) \rightarrow F(\omega, \tau_3)$ and the numerical factors for these latter two F's add to give $2/9 + 19/36 = 3/4$.

Relaxation in 2,5-DTHB-OD and 2.4-DTHB-OD

The total relaxation rate for the two molecules of interest is[2]

$$R = R_A + R_B \quad (6)$$

with

$$R_i = (9/21) \, R_i^{\text{inter}} + \sum_{j=1}^{3} (3/21) \, R_{ij}^{\text{intra}} , \quad (7)$$

where $i = $ A labels the 4-*tert*-butyl group in 2,4-DTHB-OD and the 5-*tert*-butyl group in 2,5-DTHB-OD and $i = $ B labels the 2-*tert*-butyl group in both molecules. The summation index j labels the three methyls in the ith type of *tert*-butyl group. The factors 9/21 and 3/21 are the ratios of the number of protons involved in the motion to the total number of protons in the molecule. This approach assumes that spin diffusion is rapid.[10] This is found to describe adequately the relaxation process in a wide variety of systems.[2,5,10,11] We also assume in this analysis that the relaxation is exponential. This was always found to be the case in the experiments reported here. Nonexponential relaxation is quite common in systems where only methyl reorientation occurs and this phenomenon is well understood.[12–14] However, if the methyl reorientation axes are themselves reorienting, such as the case in a *tert*-butyl group, the nonexponentiality is generally not observed.[14]

R_A describes the relaxation rate for the *tert*-butyl group with ring protons as nearest neighbors on both sides. Considering only nearest neighbor electrostatic interactions in determining the symmetry properties of the rotors, we conclude that all three methyls reorient at the same rate. Further, the magnitude of the single Zeeman relaxation rate maximum in 1,4-di-*tert*-butylbenzene (2,5-DTHB with OH replaced by H) shows unambiguously that the three methyls reorient at the same rate as the *tert*-butyl group.[5] (This is reasonable because the methyls must gear around the neighboring ring protons as the *tert*-butyl group reorients, though such classical arguments must be treated with caution.) This interpretation will turn out to be the only possible one for the 5-*tert*-butyl group in 2,5-DTHB. With the subscript "A" referring to this *tert*-butyl group and the subscript "a" referring to the constituent methyls, Eq. (7) becomes

$$R_A = (9/21) \, R_A^{\text{inter}} + (9/21) \, R_{Aa}^{\text{intra}} , \quad (8)$$

where the three terms contributing to the sum over j in Eq. (7) are equal. The intramolecular symmetry for the 2-*tert*-butyl group is lower because the ring neighbors are a hydroxy group on one side and a proton on the other. Experiments in several related molecules[2,4,15,16] show that in this case the equilibrium structure of the *tert*-butyl group has one methyl (labeled b) in the plane of the ring next to the ring proton and the other two (labeled c) out of the plane of the ring nearer the OD group. In this case, we refer to the *tert*-butyl group as a B type. The constituent b-type methyl group reorients at the same rate as the B-type *tert*-butyl group. The c-type methyls are generally freer and reorient more quickly. In this case Eq. (7) becomes

$$R_B = (9/21) \, R_B^{\text{inter}} + (3/21) \, R_{Bb}^{\text{intra}} + (6/21) \, R_{Bc}^{\text{intra}} . \quad (9)$$

Using Eqs. (1) and (4) in Eqs. (8) and (9),

TABLE I. Theoretical relaxation constants K_i and fitted multipliers A_i for 2,5-DTHB-OD.

i	K_i (10^9 s^{-2})	A_i (BPP)	A_i (DC)	A_i (Frölich)
a	1.15	1.00	1.00	$\cdots$
aa	1.15	1.00	1.00	$\cdots$
b	0.825	1.07	2.11	$\cdots$
bb	0.383	1.07	2.11	$\cdots$
c	0.322	1.17	1.31	$\cdots$
bc	0.766	1.17	1.31	$\cdots$
α	2.18	1.00	1.00	0.83
β	1.15	1.07	2.21	1.30
γ	1.09	1.17	1.28	1.77

$$R_A = R_a + R_{aa}$$
$$= K_a \, F(\omega, \tau_a) + K_{aa} \, F(\omega, \tau_a/2), \qquad (10)$$
$$R_B = R_b + R_{bb} + R_c + R_{bc}$$
$$= K_b F(\omega, \tau_b) + K_{bb} F(\omega, \tau_{b/2})$$
$$+ K_c F(\omega, \tau_c) + K_{bc} F(\omega, \tau_{bc}). \qquad (11)$$

The numerical constants K_i are given in Table I. The correlation times have been written

$$\tau_2^A = \tau_a ,$$
$$\tau_3^{Aa} = \tau_a ,$$
$$\tau_{23}^{Aa} = \{(\tau_2^A)^{-1} + (\tau_3^{Aa})^{-1}\}^{-1} = \tau_a/2 ,$$
$$\tau_2^B = \tau_b ,$$
$$\tau_3^{Bb} = \tau_b , \qquad (12)$$
$$\tau_{23}^{Bb} = \{(\tau_2^B)^{-1} + (\tau_3^{Bb})^{-1}\}^{-1} = \tau_b/2 ,$$
$$\tau_3^{Bc} = \tau_c ,$$
$$\tau_{23}^{Bc} = \{(\tau_2^B)^{-1} + (\tau_3^{Bc})^{-1}\}^{-1}$$
$$= \{(\tau_b)^{-1} + (\tau_c^{-1})\}^{-1} \equiv \tau_{bc} .$$

THE SPECTRAL DENSITY

The spectral density function $j(\omega,\tau)$ in Eqs. (10) and (11) [via Eq. (3)] provides the connection between theory and experiment. The form of $j(\omega,\tau)$ is an important and unsolved problem in dynamic magnetic resonance. It is closely related to the general line shape problem in magnetic resonance spectroscopy.[1] Although we take a phenomenological approach here, we note that this leads to new insights into the more general problem.[3,17] Of the many phenomenological spectral densities available,[2,18–20] we use three; some for the purpose of instruction and others to fit the data.

If we assume that the intramolecular dynamics is described by Poisson statistics, $j(\omega,\tau)$ is a Lorentzian in τ;

$$j(\omega,\tau) = 2\tau/(1 + \omega^2\tau^2). \qquad (13)$$

This is the Bloembergen–Purcell–Pound (BPP) spectral density[21] and is characterized by a unique τ. The Davidson–Cole (DC) spectral density[22] is

$$j(\omega,\tau) = \frac{2}{\omega} \frac{\sin(\epsilon \tan^{-1} \omega\tau)}{(1 + \omega^2\tau^2)^{\epsilon/2}} . \qquad (14)$$

It incorporates a distribution of correlation times characterized by a width parameter ϵ and a cut-off correlation time τ. As $\epsilon \to 1$, $j(\omega,\tau)$ in Eq. (14) becomes the BPP function in Eq. (13). The DC spectral density is one of the simplest closed-form expressions for $j(\omega,\tau)$ that predicts the frequently observed ω dependence of R.[5]

In this study we assume that intramolecular reorientation is thermally activated and that the various correlation times are related to effective activation energies via Arrhenius relationships,

$$\tau = \tau_\infty e^{E/kT}. \qquad (15)$$

We assume that τ_∞ is independent of temperature which is supported by the two extremes of a two-level system[23] and a continuum of levels.[24] Both models assume $E \gg kT$ which is characteristic of methyl and *tert*-butyl reorientation in molecular solids. Although there is a wide range of models for τ_∞, they all predict $10^{-14} \text{ s} < \tau_\infty < 10^{-12}$ s. (We note that we are well above the temperature region where quantum mechanical tunneling is important). In the BPP case, E is a unique activation energy characterizing the reorientation and in the DC case, it is a cutoff.

The third spectral density was introduced by Frölich[25] and generalized by us.[3]

$$j(\omega,\tau) = \frac{2kT}{\omega} \sum_{i=1}^{N} \frac{a_i}{E_{ih} - E_{il}}$$
$$\times [\tan^{-1}(\omega\tau_{ih}) - \tan^{-1}(\omega\tau_i)]. \qquad (16)$$

The correlation times $\tau_{i\rho}$, $\rho = h,l$ are given by Eq. (15) with parameters $E_{i\rho}$ and $\tau_{\infty i\rho}$. We assume that $\tau_{\infty i\rho} = \tau_{\infty l}$ is independent of ρ. The spectral density in Eq. (16) arises from a distribution of BPP spectral densities where the distribution function is made up of a histogram of N constants of value $a_i/(E_{ih} - E_{il})$; $i = 1$ to N. Thus E_{il} and E_{ih} are lower and upper cutoff energies for the ith box. The constants a_i are weights constrained by $\Sigma_i a_i/(E_{ih} - E_{il}) = 1$.

RESULTS AND DISCUSSION

The R vs T and ω data for the two isomers of DTHB are difficult to interpret quantitatively so they provide a unique opportunity to investigate the adequacy of different spectral density functions. We first assign the various motions to the relaxation peaks (R maxima) for 2,5-DTHB-OD. The low temperature peak (labeled α in Fig. 2) arises from $\omega\tau_a \sim 1$ for the A-type 5-*tert*-butyl group and its three constituent a-type methyl groups. The high-temperature peak (labeled β) arises from $\omega\tau_b \sim 1$ for the B-type 2-*tert*-butyl group and its constituent b-type methyl group (in the plane of the ring adjacent to the neighboring ring proton). The γ peak arises from $\omega\tau_c \sim 1$ for the c-type methyl groups in the B-type *tert*-butyl group [above and below the plane of the ring adjacent to the OH (or OD) group]. This R_{max} assignment is independent of the detailed form of the spectral density chosen to interpret the data. The assignments are made on the basis of several observations. First, it is the only one consistent with several other closely related molecules.[2–6,15–17] Second, the maximum values of R associated with the β and γ peaks are of similar magnitude and they are about one-half the value of
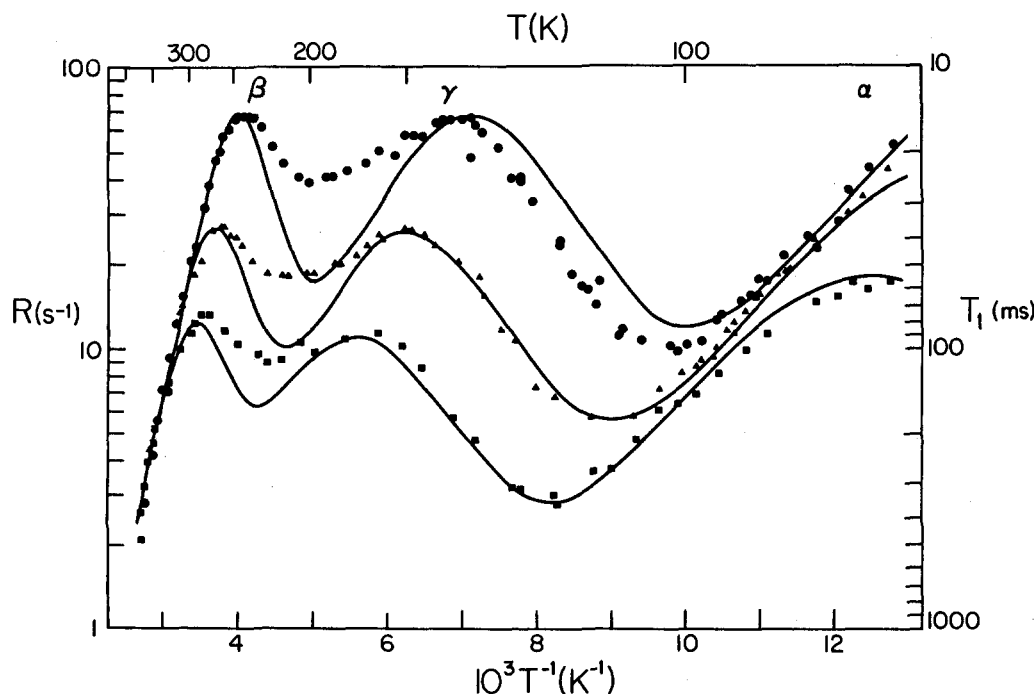
FIG. 4. Measured R vs T in 2,5-DTHB-OD at $\omega/2\pi = 8.50$ (circles), 22.5 (triangles), and 53.0 MHz (squares). The solid line is a fit to the BPP spectral density as discussed in the text. The details of the fit at high T are shown in Fig. 5.

R_{max} for the α peak at 53 MHz which is the only frequency where the α peak R_{max} is observed. This is predicted by the above interpretation and is observed in related molecules.[4,5,15,16] Third, comparison of R vs T^{-1} data for the 2,5-DTHB-OH and -OD molecules shows that R is substantially larger for the protonated molecule on the low temperature side of the γ peak. The magnitude of the difference suggests both that the OH group reorients with $\omega\tau \sim 1$ in this temperature range and that the OH motion provides an additional relaxation mechanism for the c-type methyls in the B-type t-butyl group. This result is observed in other molecular systems with B-type t-butyl groups.[4,5,16]

There is no significant difference between R vs T^{-1} in 2,4-DTHB-OH and 2,4-DTHB-OD at either 8.50 and 53.0 MHz (Fig. 3), indicating that the OH group in this molecule
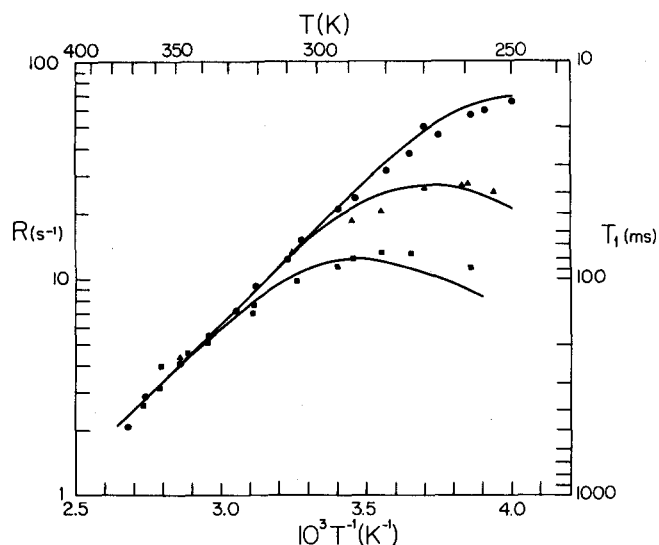

FIG. 5. Measured high temperature R vs T in 2,5-DTHB-OD at $\omega/2\pi =$ 8.50 (circles), 22.5 (triangles), and 53.0 MHz (squares). The solid line is a fit to the BPP spectral density as discussed in the text.

does not reorient on the Larmor period time scale. Because of the time dependence of proton–proton distances, the presence of the OH group complicates quantitative interpretation of the data so we restrict our present discussion to 2,5-DTHB-OD.

Figures 4 and 5 show an example of a fit of the R vs T^{-1} data for 2,5-DTHB-OD using the BPP spectral density. Quantitative agreement between theory and experiment is generally poor outside the regions chosen to fit the data, but the frequency dependence of the R_{max} is reproduced quite well. The six K_i are expressed as $A_i K_i$. The K_i are held at their theoretical values so the A_i, given in Table I, become the fitting parameters. The parameters $\tau_{\infty i}$ are given in Table II in the column labeled "experiment 6-term BPP" and the E_i are given in Table III. The value of $E_a = 6.2$ kJ/mol, characterizing the activation energy for the A-type t-butyls and their constituent a-type methyls, is low. This suggests a crystal structure which leaves the bulky t-butyl group relatively free. A more typical $E_a = 34$ kJ/mol is found in 1,4-di-*tert*-butylbenzene which has two A-type t-butyl groups.[5] The fitted values of the A_i (Table I) range from 1.00 to 1.17. This suggests that intermolecular dipole–dipole interactions (as well as other intramolecular dipole–dipole interactions not included in the calculated value of the K_i) contribute little to the relaxation. The value of $A_a = A_{aa} = 1.00$ is consistent with the low activation energy of 6.2 kJ/mol and suggests a relatively large distance from protons in neighboring molecules. The value of $\tau_{\infty a}$ is the same as that predicted by simple models for thermally activated rotors[23,24] (Table II). The range of values predicted by simple models exceeds the fitted value of $\tau_{\infty b}$ (for the b-type methyls in the B-type *tert*-butyls) by a factor of about 5–10. Also, these theoretical values are smaller than the fitted values of $\tau_{\infty c}$ (for the c-type methyls in the B-type t-butyls) by a factor of about 10. In addition, the fits are poor in regions where the terms involving τ_b and τ_c dominate.

TABLE II. Theoretical and experimental $\tau_{\infty}i$ values for 2,5-DTHB-OD.

i	$\tau_{\infty}i(10^{-13}\,s)$										
	Theory CH$_3$			Theory C(CH$_3$)$_3$			Experiment				
	Simple model (Ref. 23)	Triangle model (Ref. 24)	Square model (Ref. 24)	Simple model (Ref. 23)	Triangle model (Ref. 24)	Square model (Ref. 24)	Six term BPP	Three term BPP	Six term DC	Three term DC	Three term Frölich
a	2.1	2.8–3.0	1.6–1.8	8.3	11–12	6.0–7.1	2.3	1.8	3.0	2.3	2.2
b	1.0	1.3–1.3	0.85–1.1	3.9	4.9–5.2	3.3–4.3	0.19	0.15	0.34	0.27	0.80
c	1.7	2.2–2.6	0.78–1.6	⋯	⋯	⋯	23	23	1.1	1.1	0.80

Although the BPP spectral density does not adequately fit the data, it is qualitatively correct; it contains the salient features of what a more precise model would predict. We shall use these fits to investigate the relationships between and the relative importance of the various relaxation terms in Eqs. (10) and (11). In Fig. 6, we plot the six terms in Eqs. (10) and (11) as well as different linear combinations. The $R_a + R_{aa}$ [Eq. (10)] and $R_b + R_{bb}$ [part of Eq. (11)] separation is easily understood; the former involves τ_a and $\tau_a/2$ and the latter involves τ_b and $\tau_b/2$. The R_{bc} term which involves $(\tau_b^{-1} + \tau_c^{-1})^{-1} = \tau_c(1 + \tau_c/\tau_b)^{-1}$ may be replaced by τ_c for $\tau_b \gg \tau_c$, which is true over the entire temperature range studied here. Thus the two terms in $R_c + R_{bc}$ are conveniently linked together. Although an unnecessary approximation for many spectral densities, it is simpler to replace the six distinct terms in Eqs. (10) and (11) with three terms. We define

$$R_{\alpha} = R_a + R_{aa} = K_{\alpha}F(\omega,\tau_a),$$
$$R_{\beta} = R_b + R_{bb} = K_{\beta}F(\omega,\tau_b), \qquad (17)$$
$$R_{\gamma} = R_c + R_{bc} = K_{\gamma}F(\omega,\tau_c),$$

where the K_j are given in Table I. R_{α}, R_{β}, and R_{γ} are shown in Fig. 6. This is an excellent approximation for R_{γ} where $K_{\gamma} = K_c + K_{bc}$ since $\tau_{bc} \simeq \tau_c$. Also, $K_aF(\omega,\tau_a) + K_{aa}F(\omega,\tau_a/2)$ can be approximated by $K_{\alpha}F(\omega,\tau_a)$ with K_{α} given in Table I. The new $\tau_{\infty a}$ changes to the value labeled "three-term BPP" in Table II and E_a does not change. The same analysis applies to K_{β}, $\tau_{\infty b}$, and E_b. We can now replace Eqs. (10) and (11) with

$$R_A = R_{\alpha} = K_{\alpha}F(\omega,\tau_a),$$
$$R_B = R_{\beta} + R_{\gamma} = K_{\beta}F(\omega,\tau_b) + K_{\gamma}F(\omega,\tau_c), \qquad (18)$$

and the resultant three-term BPP fit is indistinguishable

TABLE III. Values of the parameter E_i.

i	E_i (kJ/mol)			
	2,5-DTHB			2,4-DTHB
	BPP	CD	Frölich	Frölich
a	6.2	6.2	6.2	3.3–16
b	28	28	22–25	12–26
c	10	15	12–18	6.7–15

from the six-term BPP fit.

The BPP spectral density fails to explain the frequency dependence of R on the low temperature side of the γ peak. Subtracting off the α relaxation, R vs ω in this region varies as $\omega^{1.6}$ whereas BPP theory predicts ω^2. An ω^n dependence for R with $n < 2$ is predicted by several spectral density formalisms,[17] a tractable example of which is the DC spectral density given by Eq. (14). It predicts $R \propto \omega^{1+\epsilon}$ for $\omega\tau \gg 1$. A fit of the data using the DC spectral density is shown in Fig. 7. The DC spectral density includes four adjustable parameters, the three already encountered in BPP theory A_i, E_i, and $\tau_{\infty i}$ plus ϵ_i which provides a measure of the width of the distribution of correlation times. The A_i, E_i, and $\tau_{\infty i}$ are given in Tables I–III for both the six-term DC fit using Eqs. (10) and (11) with Eqs. (3), (14), and (15) and for the 3-term DC fit using Eqs. (18) with Eqs. (3), (14), and (15). The width parameters, which are the same for both the six-term and the three-term fit are $\epsilon_a = 0.75$; $\epsilon_b = 0.30$, and $\epsilon_c = 0.60$. The DC spectral density fits the α-peak for the A-type *tert*-butyl group better than the BPP spectral density, but the difference is negligible. The parameters A_a and E_a do not change. The parameter $\tau_{\infty,a}$ which increases by about 20% remains of the order of magnitude predicted by simple theories.[23,24] The fits for the β and γ peaks in Fig. 7 are better than those obtained with a BPP spectral density (Fig. 4). The parameter E_c for the c-type methyls changes from 10 kJ/mol in the BPP fit to 15 kJ/mol in the DC fit because the low-temperature slope is E/k for the former and $\epsilon E/k$ for the latter. The parameter $\tau_{\infty c}$ is reduced by a factor of 20 which brings it into line with the simple theories[23,24] (Table II). The excellent agreement between theory and experiment in the vicinity of the γ peak at all three frequencies is evidence that the interpretation of τ_c in terms of its constituent parameters E_c and $\tau_{\infty c}$ adequately explains the dynamics of the c-type methyls. The parameter A_c (A_{γ}) is 1.3, suggesting non-negligible, non-intra-*tert*-butyl spin–spin dipolar interactions. Perhaps the c-type methyls are more sensitive to neighboring molecules because they lie in and out of the plane of the aromatic ring. There are no nearby ring protons on the same molecule.

Although the fit of the high temperature β peak is satisfactory if not excellent, the fitted value of $A_b = 2.1$ (Table I) is difficult to interpret, especially since $A_b = 1.1$ for the BPP fit. The strength of the dipolar couplings are proportional to r^{-6} and barring some very strange crystal structure, approximate calculations show that it is impossible for non-
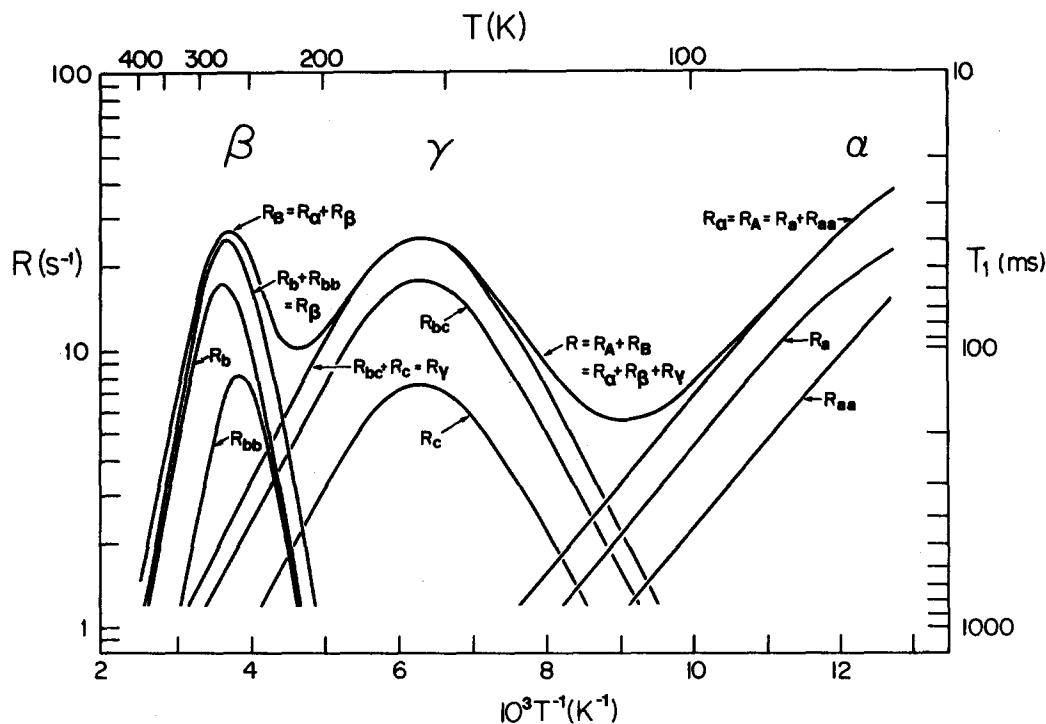
FIG. 6. Theoretical R vs T in 2,5-DTHB-OD at $\omega/2\pi = 22.5$ MHz. The theoretical curves show the various contributions to the relaxation rate. The R_i in the figure are defined by Eqs. (10), (11), and (17). A BPP spectral density is used.

intra-*tert*-butyl interactions to contribute as much to the relaxation as intra-*tert*-butyl intractions which is what $A_b = 2$ implies. Also, the fitted value of $\tau_{\infty,b}$ remains considerably smaller than that predicted by the simple motional models. We conclude that this model does not adequately explain the dynamics of the 2-*tert*-butyl group and its constituent b-type methyl group, in spite of the good fit. If this high-temperature motion did not have to relax the rapidly reorienting 5-*tert*-butyl group then this A value would be reduced to about 1, which is unrealistic. There was no observation of nonexponential relaxation because the 5-*tert*-butyl group was not being relaxed nor was there a reduction of signal amplitude at high temperatures because the spins in the 5-*tert*-butyl

group were not being excited by the rf pulses. As in all of these types of molecular solids, all experiments indicate rapid spin diffusion. The failure of the BPP and DC spectral densities for this high-temperature motion has important ramifications. Both spectral densities are normalized and the important result is that the theory does not predict sufficient relaxation intensity in this temperature range.

In Fig. 8, we fit the 2,5-DTHB-OD R vs T and ω data using the Frölich spectral density. We attempted to reproduce the three-term DC fit in Fig. 7 using Eq. (18) with Eqs. (3), (15), and (16). One term [$N = 1$ in Eq. (16)] was used for each of the three rotor types. Each term has parameters τ_∞, E_h, E_l, and A. The A are given in Table I, the τ_∞ are
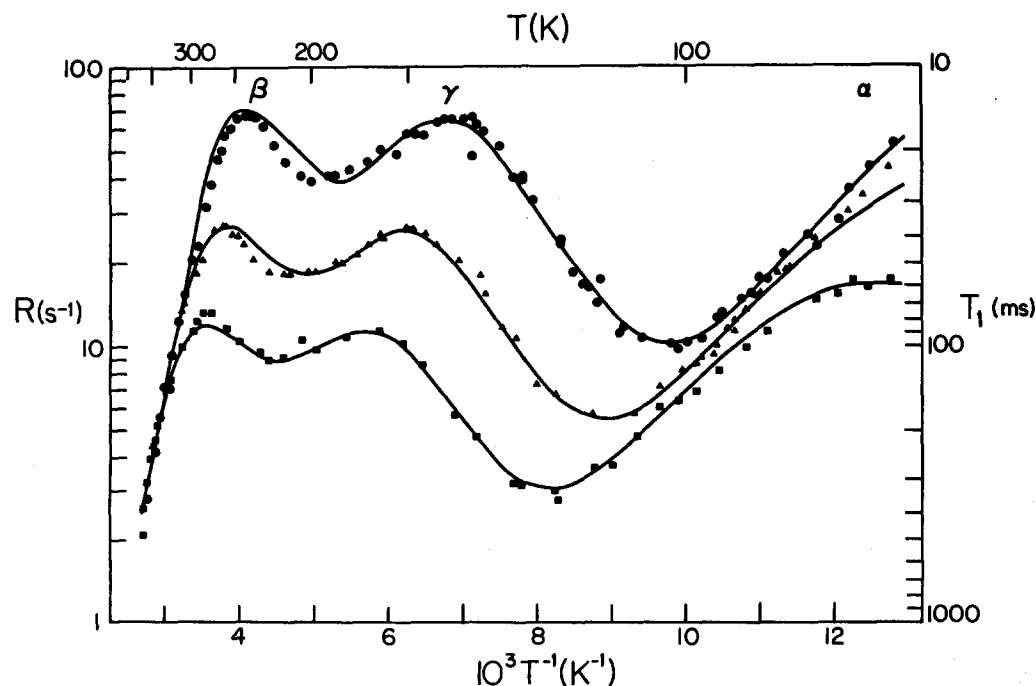

FIG. 7. Measured R vs T in 2,5-DTHB-OD at $\omega/2\pi = 8.50$ (circles), 22.5 (triangles), and 53.0 MHz (squares). The solid line is a fit to the Davidson–Cole spectral density as discussed in the text.
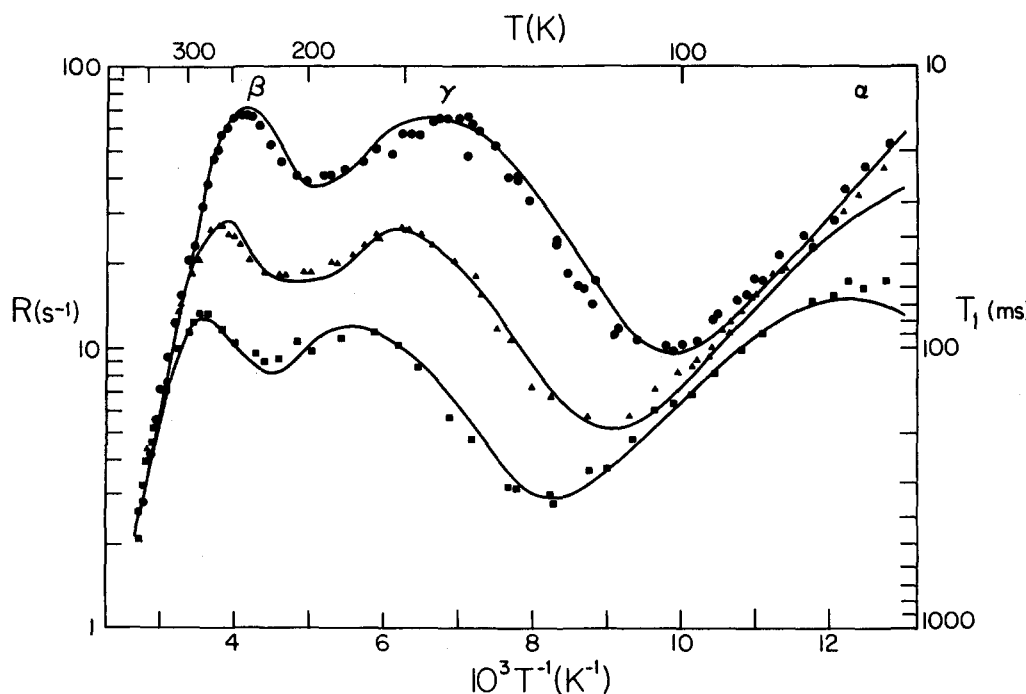
FIG. 8. Measured R vs T in 2,5-DTHB-OD at $\omega/2\pi = 8.50$ (circles), 22.5 (triangles), and 53.0 MHz (squares). The solid line is a fit to the Frölich spectral density with activation energy distributions as shown in Fig. 9.

given in Table II, and the E_l and E_h are indicated as a range E_l-E_h in Table III. The E_l and E_h are also indicated in Fig. 9 which shows the normalized distribution functions $\Gamma(E)$ characterizing the rotational properties of the three types of rotors. Since the BPP spectral density fit the α peak quite satisfactorily, a Dirac δ function can be used for this case.

It is interesting that such a simple distribution of BPP spectral densities will fit the data so well. The three constant distribution functions in Fig. 9 reproduce quite adequately the R vs T and ω from using the DC spectral density. Since the DC spectral density employs a distribution of correlation times and the Frölich spectral density employs a distribution of activation energies, it is not easy to relate them in a general way. We shall address this in the future.

To show how the data for the 2,4-isomer can be interpreted in the same fundamental manner as the 2,5-isomer, we broaden the distributions of activation energies used to interpret the 2,5-isomer. For the purposes of comparison, the 8.5 MHz fit for 2,5-DTHB in Fig. 8 is reproduced by the solid line on the 2,4-DTHB data in Fig. 10. The dashed-dotted line in Fig. 10 shows the result of lowering all the

E_l/k and raising all the E_h/k of Fig. 9 by 1000 K. This increases $\Delta E = E_h - E_l$ by 8.4 kJ/mol. As an example, for the solid line, the α relaxation term corresponds to $E_{al} = E_{ah}$ = 6.2 kJ/mol with $\Gamma(E_a) = \delta(E_a - 6.2$ kJ/mol). For the dashed-dotted line, $E_{al} = 2.0$ kJ/mol and $E_{ah} = 10.4$ kJ/mol with $\Gamma(E_a) = (10.4 - 2.0$ kJ/mol$)^{-1} = 0.12$ mol/kJ;
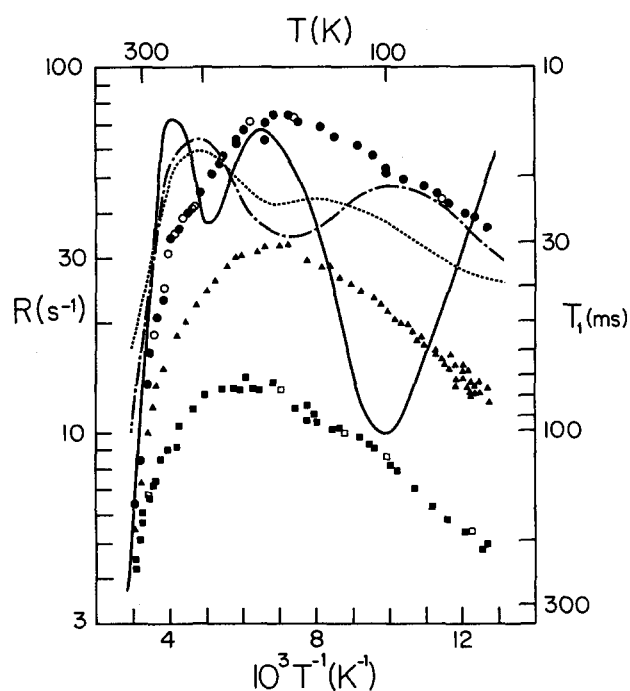

FIG. 10. Measured R vs T in 2,4-DTHB. The symbols are explained in the caption to Fig. 3. The theoretical lines follow from using the Frölich spectral density as discussed in the text. The solid line is that used for 2,5-DTHB in Fig. 8 which, in turn, employs the distribution of activation energies shown in Fig. 9. The dashed-dotted line is obtained by widening these three distributions by 8.3 kJ/mol. The dotted line is obtained by widening these distributions by a further 8.3 kJ/mol but with a 0.8 kJ/mol lower limit.
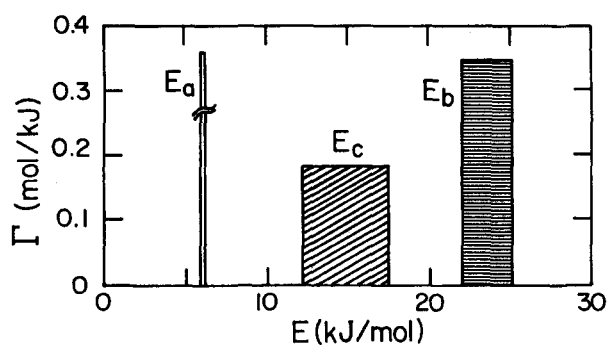

FIG. 9. The normalized distributions of activation energies used in the fit for R vs T and ω for 2,5-DTHB-OD in Fig. 8. $\Gamma(E_a)$ is a Dirac δ function and is indicated schematically.
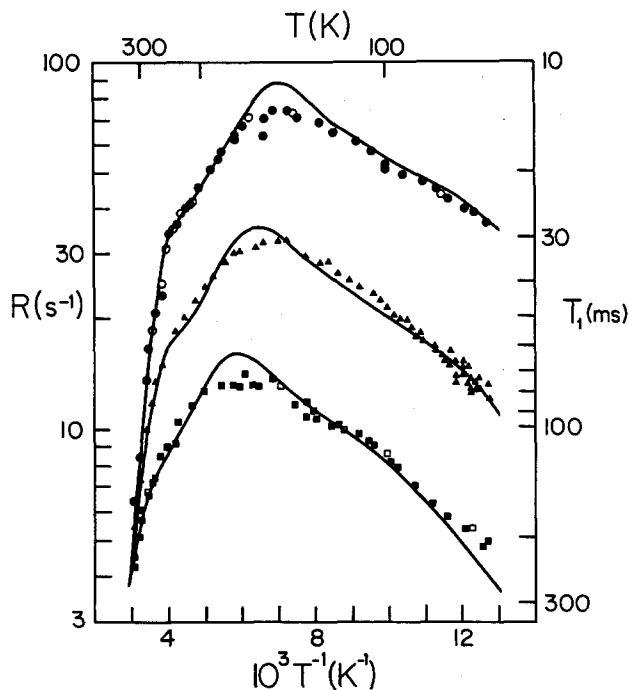
FIG. 11. Measured R vs T in 2,4-DTHB. The symbols are explained in the caption to Fig. 3. The solid line is a fit to the Frölich spectral density with activation energy distributions as shown in Fig. 13. The high temperature portion is expanded in Fig. 12.

FIG. 13. The normalized distributions of activation energies in the fit R vs T and ω for 2,4-DTHB in Figs. 11 and 12.

intensity (i.e., the area under $\ln R$ vs T^{-1}) is generally reproduced by this approach.

The theoretical curves in Fig. 10 for the 2,4-isomer result from taking the best fits for the 2,5-isomer and systematically changing a single parameter. Figures 11 and 12 show a fit to the 2,4-DTHB data varying fitting parameters $\tau_{\infty i}$, E_{il}, and E_{ih} $(i = a,b,c)$, but keeping the A_i ($i = \alpha, \beta, \gamma$) at the values found for 2,5-DTHB in Fig. 8. Although there are several adjustable parameters, we emphasize the severe constraint on the fitting procedure produced by fixing the strength parameters A_i. The resulting fit is good, particularly the reproduction of the "knee" at ~ 250 K (Fig. 12). There is considerable overlap among the three distributions used in this fit as shown in Fig. 13, which explains the lack of distinction among the three peaks. The success in the fits for 2,4-DTHB may be taken to suggest that the three types of rotors retain their identity to some degree.

The rotors in 2,4-DTHB can be characterized by a single distribution function, $AK\Gamma(E)$ (Fig. 14) which is plotted from the sum $\Sigma_{i=1}^{3} A_i K_i \Gamma(E_i)$. The A_i and K_i are taken from Table I and the $\Gamma(E_i)$ from Fig. 13. The histogram in Fig. 14 may be replaced by a continuous distribution. We are exploring this possibility because this will reduce the number of parameters needed to fit the data.

2.0 kJ/mol $< E_a <$ 10.4 kJ/mol, $\Gamma(E_a) = 0$ otherwise. The E_b and E_c distributions in Fig. 9 were broadened by the same constant amount. This broadens the β and γ relaxation peaks to the point where they are no longer resolved but the α peak at ~ 100 K is still distinct at the Larmor frequency of $\omega/2\pi = 8.50$ MHz used for these sample calculations. A further broadening of 4.2 kJ/mol (with lower limits of 0.8 kJ/mol) results in the dotted line in Fig. 10. The α peak remains identifiable at ~ 120 K, but barely. We note that the
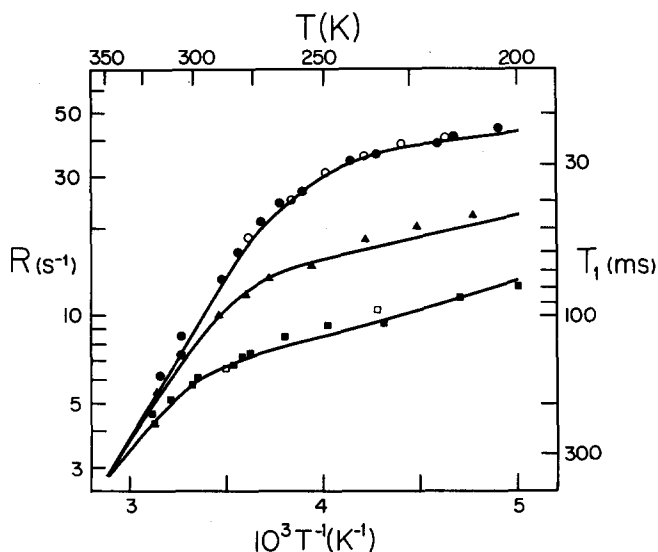

FIG. 12. Measured high temperature R vs T in 2,4-DTHB. The symbols are explained in the caption to Fig. 3. The solid line is discussed in the caption to Fig. 11.
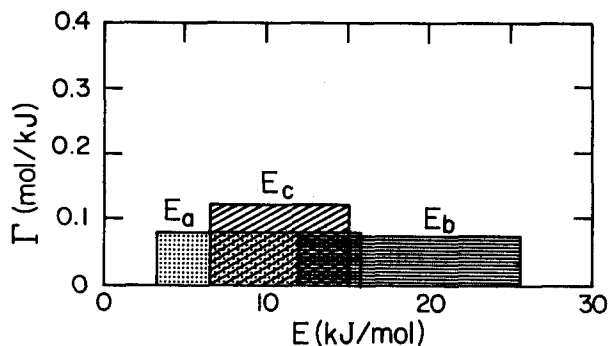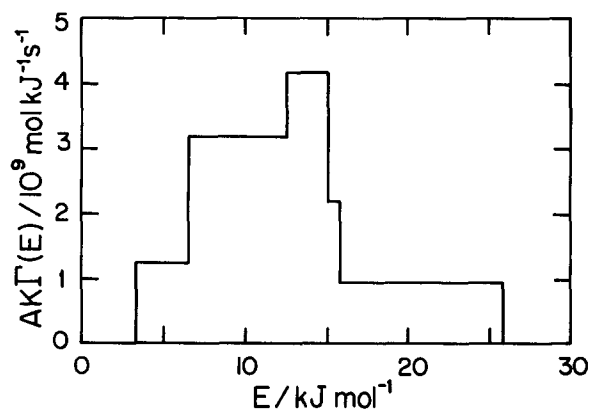

FIG. 14. The relaxation weight $AK\Gamma(E)$ as a function of activation energy E for 2,4-DTHB deduced from the distribution in Fig. 13 and the parameters A and K Table I.

CONCLUDING REMARKS

We have discussed the Zeeman relaxation rate R in molecular solids where the relaxation results from the modulation of nuclear dipole–dipole interactions by the reorientation of *tert*-butyl groups and their constituent methyl groups.[1] We reviewed the general theory which separates the reorienting groups into symmetry types.[2] A distinctive maximum in R usually results when $\omega\tau \sim 1$ for each rotor type. This approach works well for a very wide variety of molecular solids[2–5,15–17] including 2,5-DTHB which we have investigated in this paper. The frequency and temperature dependence of R can generally be fitted with standard spectral densities[2,18–20] and the models usually predict a distribution of correlation times.

In some molecules which have only one rotor type, like 3,5-DTHB, the distributions can become very wide.[3] This phenomenon becomes very interesting when there are different rotor types since in this case the distributions of correlation times can become so wide that the individual rotor types lose their distinction. This is the case for 2,4-DTHB which is also reported in this paper. We have shown that the relaxation data for 2,4-DTHB can be interpreted by broadening the three relatively narrow distributions describing the reorientation of the three rotor types in 2,5-DTHB. The data can also be interpreted by assuming a very wide range of activation energies for a single rotor type. We are proceeding with both theoretical and experimental studies to determine the origin of this distribution of correlation times for intramolecular reorientation. In particular, a variable temperature x-ray study is needed. It is not yet clear whether there really is a distribution of exponential correlation functions, each characterized by a unique correlation time, or whether the correlation function is just highly nonexponential. This is a fundamental question about a simple process. It can be clarified by comparing similar molecular systems like the two isomers of di-*tert*-butylhydroxybenzene studied here.

ACKNOWLEDGMENTS

[1] C. P. Slichter, *The Principles of Magnetic Resonance* (Springer–Verlag, Berlin, 1978).

[2] P. A. Beckmann, Chem. Phys. **63**, 359 (1981).

[3] A. M. Albano, P. A. Beckmann, M. E. Carrington, E. E. Fisch, F. A. Fusco, A. E. O'Neill, and M. E. Scott, Phys. Rev. B **30**, 2334 (1984). The factor a_j should be inserted inside the summation in Eq. (5).

[4] M. C. Aronson, P. A. Beckmann, R. J. Ross, and S. L. Tan, Chem. Phys. **63**, 349 (1981).

[5] P. A. Beckmann, F. A. Fusco, and A. E. O'Neill, J. Magn. Reson. **59**, 63 (1984).

[6] P. A. Beckmann, Mol. Phys. **41**, 1227 (1980).

[7] M. B. Dunn and C. A. McDowell, Mol. Phys. **24**, 969 (1972).

[8] D. W. Larsen and J. H. Strange, J. Phys. Chem. **84**, 1944 (1980).

[9] S. Albert, H. S. Gutowsky, and J. A. Ripmeester, J. Chem. Phys. **56**, 3672 (1972).

[10] J. E. Anderson and W. P. Slichter, J. Phys. Chem. **69**, 3099 (1965).

[11] F. Köksal and S. Bahceli, Z. Naturforsch. Teil A **39**, 548 (1984).

[12] L. K. Runnels, Phys. Rev. A **134**, 28 (1964).

[13] R. L. Hilt and P. S. Hubbard, Phys. Rev. A **134**, 392 (1964).

[14] J. D. Cutnell and W. Venable, J. Chem. Phys. **60**, 3795 (1974).

[15] P. A. Beckmann, C. I. Ratcliffe, and B. A. Dunell, J. Mag. Reson. **32**, 391 (1978).

[16] M. C. Aronson, P. A. Beckmann, V. Guerra, C. M. Schwamb, and S. L. Tan, Mol. Phys. **41**, 1239 (1980).

[17] A. M. Albano, P. A. Beckmann, M. E. Carrington, F. A. Fusco, A. E. O'Neill, and M. E. Scott, J. Phys. C **16**, L979 (1983).

[18] T. M. Conner, Trans. Faraday Soc. **60**, 1574 (1964).

[19] F. Noack and G. Preissing. Z. Naturforsch. Teil A **24**, 143 (1969).

[20] F. Noack, in *NMR Basic Principles and Progress*, edited by P. Diehl, E. Fluck, and R. Kosfeld (Springer–Verlag, Heidelberg, 1971), Vol. 3, p. 81.

[21] N. Bloembergen, E. M. Purcell, and R. V. Pound, Phys. Rev. **73**, 679 (1948).

[22] D. W. Davidson and R. H. Cole, J. Chem. Phys. **19**, 1484 (1951).

[23] D. E. Woessner and B. S. Snowden, Jr., Adv. Mol. Relaxation Processes **3**, 181 (1972).

[24] S. Clough and A. Heidemann, J. Phys. C **13**, 3585 (1980).

[25] H. Frölich, *Theory of Dielectrics* (Oxford University, Oxford, 1949).